Chapter 6

NON LINEAR STRUCTURAL ANALYSIS.
APPLICATION FOR EVALUATING SEISMIC
SAFETY

Juan Carlos Vielma[a],*, Alex Barbat [b] and Sergio Oller [b]
[a] Lisandro Alvarado University
[b] Technical University of Catalonia

Keywords: Non-linear analysis, ductility, overstrength, seismic safety.

1.   Introduction

Performance-Based Design is currently accepted commonly as the most advanced design and evaluation approach. However, successful application of this procedure depends largely on the ability to accurately estimate the parameters of structural response.

Determination of these parameters requires application of analysis procedures where the main non-linear behavior features (constitutive and geometrical) of structures are included. This chapter presents and discusses these features of non-linear behavior and how they are incorporated in the process of static or dynamic structural analyses. Non-linear analysis leads to determination of significant structural response parameters whenever estimating seismic responses such as ductility, overstrength, response reduction factor and damage

---

*E-mail address: jcvielma@ucla.edu.ve

thresholds; being these the main response parameters for evaluating the seismic safety of structures. In order to illustrate application of the non-linear procedure being described, a set of concrete-reinforced moment-resisting framed buildings with various numbers of levels was selected. These buildings were designed according to ACI-318 [1] for high and very high level of seismic hazard.

Seismic safety of regular concrete-reinforced framed buildings is studied using both the static and dynamic non-linear analyses. Static analysis consists in using the pushover procedure and dynamic analysis is done by using the incremental dynamic analysis (IDA). Analysis was performed using the PLCd computer code [2] which allows incorporation of the main characteristics of reinforcement and confinement provided to the cross sections of structural elements (beams and columns). A set of 16 concrete-reinforced framed buildings with plane and elevation regularity was designed according to ACI-318 [1] and for loads prescribed by the ASCE7-05 [3]. Results obtained from static and dynamic non-linear analyses allowed calculation of global ductility, overstrength and behavior factors. Behavior factors are compared with design values prescribed by the ASCE7-05, in order to verify validity of design values.

Seismic safety of buildings has been evaluated using an objective damage-index obtained from the capacity curve, computed for normalized roof displacements corresponding to performance point. Additionally, five damage thresholds are defined using the values of inter-story drifts associated with several Limit States. Damage thresholds lead to obtain fragility curves and damage probability matrices, used in order to evaluate the seismic safety of the code-designed buildings under study.

2.   Seismic Design of Buildings

The main objective of the seismic design is to obtain structures capable of sustaining a stable response under strong ground motions. Some aspects of the current seismic analysis procedures allow for adapting non-linear features into an equivalent elastic analysis and, obviously, formulation of these procedures is essential for assuring a satisfactory earthquake-resistant design.

In earthquake-resistant engineering, stable behavior is achieved through compliance with conceptual design, thus implying regularity of the structure both in plane and elevation as well as continuity of resistant elements to lateral loads. It is also essential that the structure elements are able to dissipate energy, reaching damage levels which do not threaten the stability of the structure as a
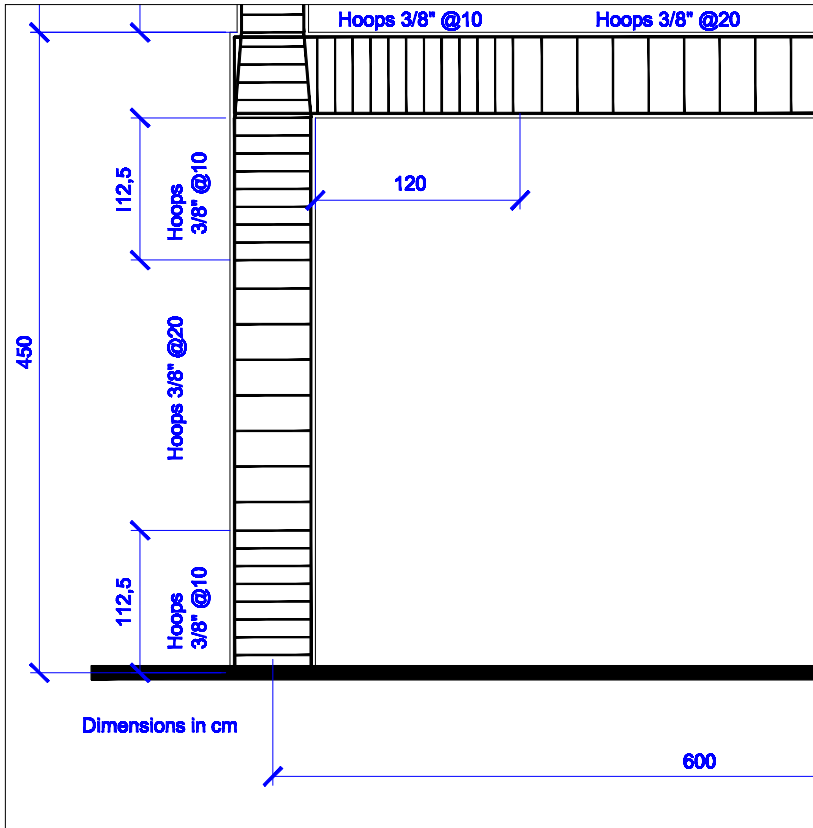
Figure 1. Typical reinforcement in beam-column special zones.

whole. In order to achieve this global behavior in concrete-reinforced buildings it is necessary to supply proportional confinement in special zones of beams and columns, finding these zones near to beam-column joints, see Figure 1.

It is especially interesting to know the seismic behavior of code-designed buildings. In order to study the behavior of low and medium vibration periods, a set of regular concrete-reinforced moment-resisting framed buildings (MRFB) designed according to ACI-318 were analyzed. Low and medium period responses were obtained by considering variable number of stories (3, 6, 9 and 12). Structural redundancy was included varying spam number (3, 4, 5 and 6). For each building structure, inner and outer frames were defined to the corre-
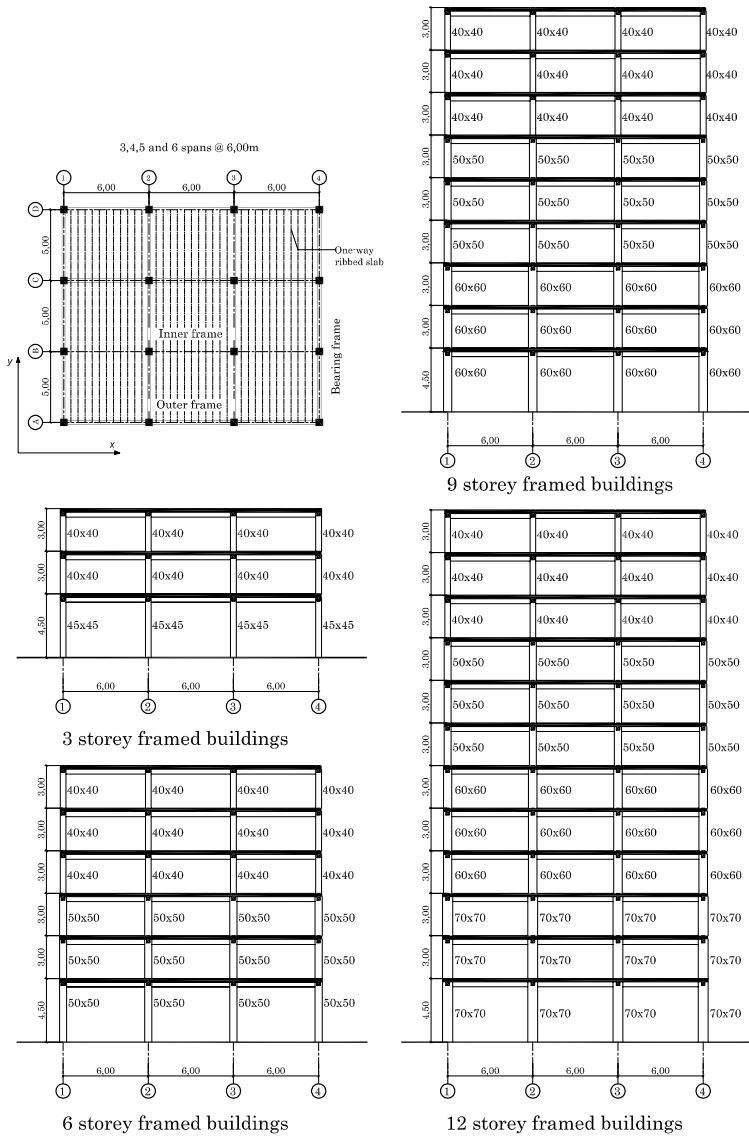
Figure 2. Plan and elevation views of designed buildings.

sponding load ratio (seismic load/gravity load). Frame members were analyzed, designed and detailed following the code prescriptions for special moment- resisting frames (high ductility level). Seismic demand is defined for type B soil (stiff soil) and for a peak ground acceleration of 0.3g and 0.4g. Geometric characteristics of typical frames are shown in Figure 2.

Non-linear analysis procedures have been used in previous studies to assess the seismic design of buildings designed according to specific design codes [4–6]. Static incremental non-linear analysis (Pushover Analysis) is an analysis procedure commonly adopted by the scientific community and practicing engineers in order to evaluate the seismic capacity of new or existing buildings. This analysis can be performed by using a predefined lateral load distribution; lateral load distribution is usually applied following a specific pattern, which corresponds to the shape of lateral displacements obtained from the modal analysis.

Dynamic analysis can be applied using an adequate set of records obtained from strong motion databases or from spectrum-compatible design synthesized accelerograms.

2.1. Seismic Response Parameters

The seismic response parameters considered most relevant in recent works are: global ductility, overstrength and behavior factor which can be calculated by applying deterministic procedures based on non-linear response of structures subject to static or dynamic loads. Although it is difficult to find a method to determine global yield and ultimate displacements [7], a simplified procedure is applied in this work.

The procedure is based on non-linear static response obtained via finite element techniques, which allows generating idealized bilinear capacity curve shape shown in Figure 3, with a secant segment from the origin to a point that corresponds to 75% of maximum base shear [8, 9]. The second segment, representing the branch of plastic behavior was obtained by finding the intersection of the aforementioned segment with another horizontal segment, corresponding to maximum base shear. Using this compensation procedure guarantees that energies dissipated by the ideal system and by the modeling one, are equal (see Figure 3).

For a simplified non-linear static analysis, there are two variables that typify the quality of seismic response of buildings. The first is global ductility μ, defined as
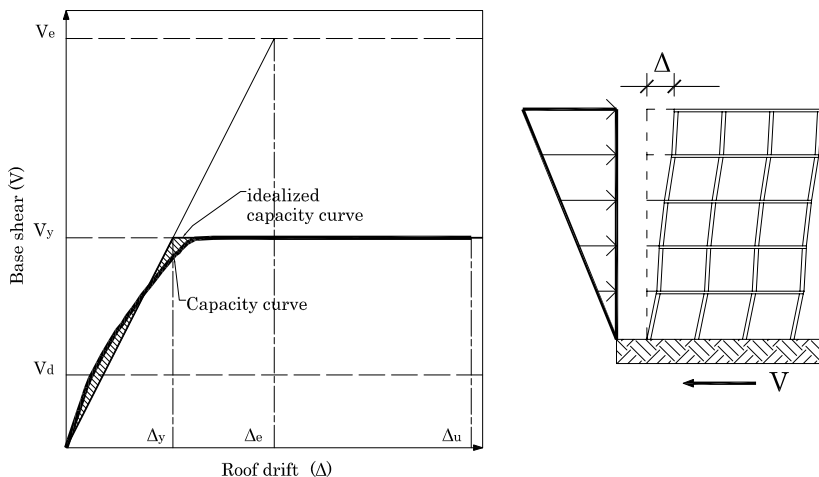
Figure 3. Scheme for determining displacement ductility and overstrength.

$$\mu = \frac{\Delta_u}{\Delta_y} \qquad (1)$$

calculated based on values of yield drift, Δ_y, and ultimate drift, Δ_u, represented in the idealized capacity curve shown in Figure 3.

Second variable is the overstrength of the building R_R, defined as ratio of yielding base shear, Vy to design base shear, Vd (see Figure 3).

$$R_R = \frac{V_y}{V_d} \qquad (2)$$

3.   Structural Modeling

In order to obtain non-linear responses of buildings, it is necessary to model the structures taking into account their geometrical and mechanical specifica- tions. Plane frames are used for static and dynamic analyses. This requires defining the different types of frames, mainly depending on the relationship between seismic and gravity loads carried on by the frames. Therefore, three types of frames are defined: outer and inner load frames, and bracing frames, see Figure 4.
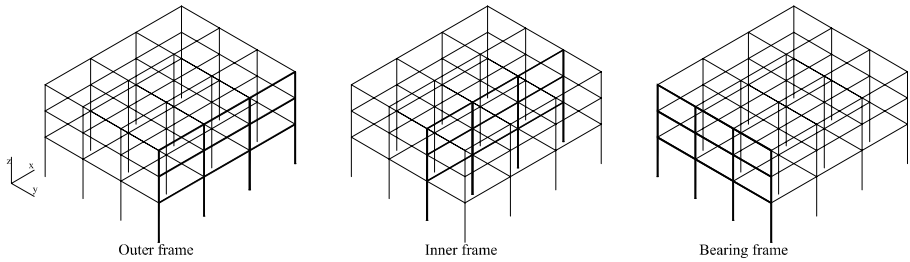
Figure 4. Definition of different building frames.

Thus frames are driscretized by taking into consideration the existence of special zones in beams and columns. This requires definition of the elements covering the length of special confined zones. Figure 5 shows a typical discretization obtained for a three stories frame.
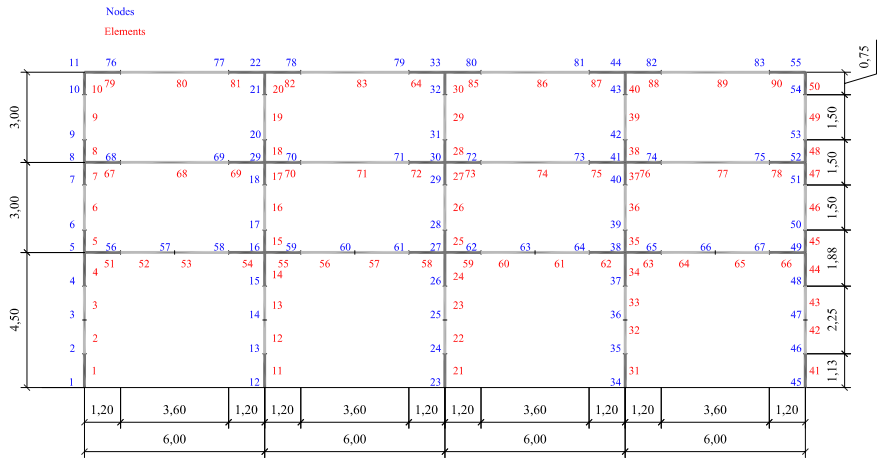

Figure 5. Frame discretization.

4.   Non Linear Analysis

Advances made in the field of non-linear structural analysis and development of improved computational tools have enabled the application of more

realistic analysis procedures for new and existent buildings, taking into account the main features of their seismic non-linear behavior, such as constitutive non-linearity (plasticity and damage) and geometrical non-linearity (large deformations and displacements).

Non-linear incremental static and dynamic analyses are performed using the PLCd finite element code [2, 10, 11]. PLCd is a finite element code which works with two and three-dimensional solid geometries as well as with prismatic, reduced to one-dimensional members. By combining both numerical precision and reasonable computational costs [12, 13] it provides a solution and it can deal with kinematics and material non-linearity. To control their evolution, it uses various 3-D constitutive laws to predict material behavior (elastic, visco-elastic, damage, damage-plasticity, etc. [14]) with different yielding surfaces (Von-Mises, Mohr-Coulomb, improved Mohr-Coulomb, Drucker-Prager, etc. [15]). Newmark's method [16] is used to perform dynamic analysis. A more detailed description of the code can be found in Mata *et al.* [12, 13]. TFor dealing with composite materials, the main numerical features included in the code are: 1) Classical and serial/parallel mixing theory is used to describe the behavior of composite components [17]. 2) 2) Anisotropy Mapped Space Theory enables the code to consider materials with a high level of anisotropy, without associated numerical problems [18]. 3) Debonding Fiber-matrix, which reduces the composite strength due to failure of reinforced-matrix interface, is also considered [19].

Experimental evidence has shown that inelasticity in beam elements can be formulated in terms of cross-sectional quantities [20] and, therefore, beam's behavior can be described by using concentrated models, sometimes called plastic hinge models, which confine all inelastic behavior at beam ends using ad-hoc force-displacement or moment-curvature relationships [21]. But in the formulation used in this computer program, the procedure consists of obtaining the constitutive relationship at cross-sectional level by integrating a selected number of points corresponding to fibers directed along the beam's axis [22]. Thus, the general nonlinear constitutive behavior is included in the geometrically exact nonlinear kinematics formulation for beams proposed by Simo [23], considering an intermediate curved-reference configuration between the straight-reference beam and the current configuration. To solve the resulting non-linear problem, displacement based method is used. Plane cross-sections remain plane after deformation of the structure; therefore, no cross sectional warping is considered, avoiding inclusion of additional warping variables in the formulation or iterative

procedures to obtain corrected cross-sectional strain fields. Thermodynamically consistent constitutive laws are used to describe the material behavior of these beam elements, thus allowing obtaining a more rational estimation of the energy dissipated by structures. The simple mixing rule for material composition is also considered when modeling materials for these elements, composed by several simple components. Special attention is paid to obtain the structural damage-index capable of describing the structure load-carrying capacity.

According to the Mixing Theory, N different components coexist in a structural element, all of them undergoing the same strain; therefore, strain compatibility is forced among material components. Free energy density and dissipation of composite are obtained as the weighted sum of free energy densities and dissipation of components, respectively. Weighting factors K_q are the participation volumetric fraction of each compounding substance, $K_q = \frac{V_q}{V}$, obtained as the quotient between the $q-th$ component volume, V_q, and total volume, V [10–13].

Discretization of frames was performed using finite elements whose lengths vary depending on column and beam zones with special confinement requirements. These zones are located near the nodes where maximum seismic demand is expected, and are designed according to general dimensions of structural elements, diameters of longitudinal steel, span length and storey heights. Frame elements are separated into equal thickness layers with different composite materials, characterized by their longitudinal and transversal reinforcement ratio (see Figure 6). Transverse reinforcement benefits are included by using the procedure proposed by Mander *et al.* [24]. This procedure consists of improving the concrete compressive strength depending on quantity and quality of the longitudinal and transversal reinforcement.

4.1.   Non Linear Static Analysis

In order to evaluate inelastic response of structures, pushover analysis was performed applying a set of lateral forces corresponding to seismic actions of the first vibration mode. Lateral forces were gradually increased starting from zero; passing through the value inducing transition from elastic to plastic behavior and finally reaching the value corresponding to ultimate drift (i.e. point at which the structure can no longer sustain any additional load and collapses). Before the structure is subject to lateral loads simulating a seismic action, it is first subject to the action of gravity loads, lumped in the nodes defined by the beam-columns joints, in concurrence with combinations applied in the elastic analysis. The
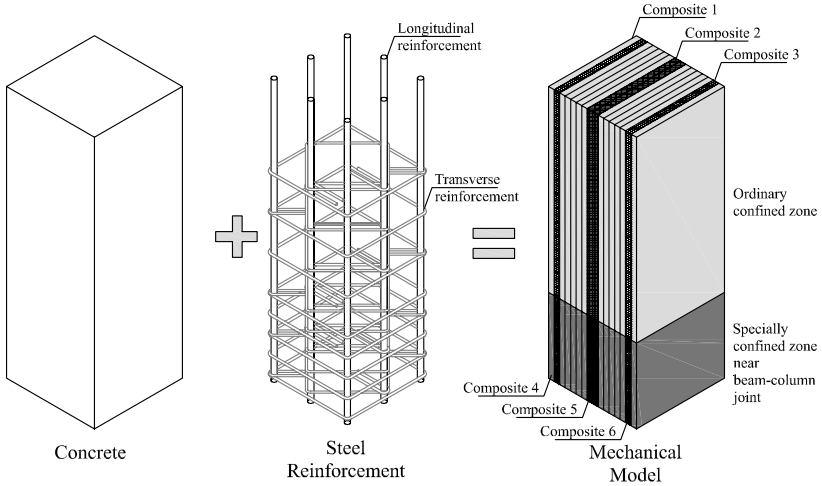
Figure 6. Discretization of RC frame elements.

method applied does not allow for evaluation of torsion effects, being the model used a 2D one. Capacity curves obtained in the analysis are shown in Figure 7.
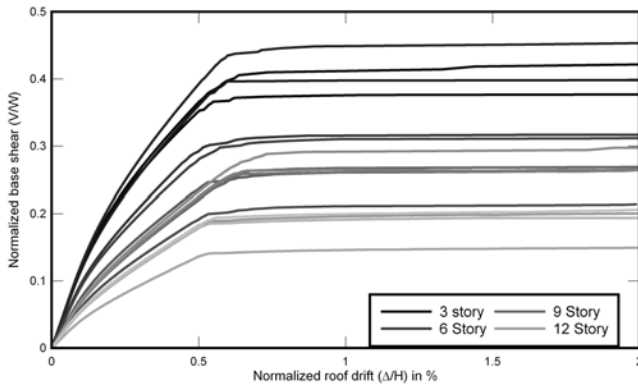

Figure 7. Capacity curves of the studied buildings.

Non-linear static analysis calculates cumulative damage in structural elements by using the procedures described in Section 4.3..Results of local damage-index at collapse displacement calculated for two of the buildings under study are shown in Figure 8. In this figure, each rectangle represents the magni-

tude of damage reached by the element. It is important to observe that for low rise buildings (N=3) the maximum values of damage correspond to the elements located at both ends of the first storey columns; this damage concentration corresponds to a soft-storey mechanism. Instead, high rise buildings (N=6, 9 and 12) show their maximum damage values at low level beam ends, according to the desired objective of conceptual design which is to produce structures with weak beams and strong columns.

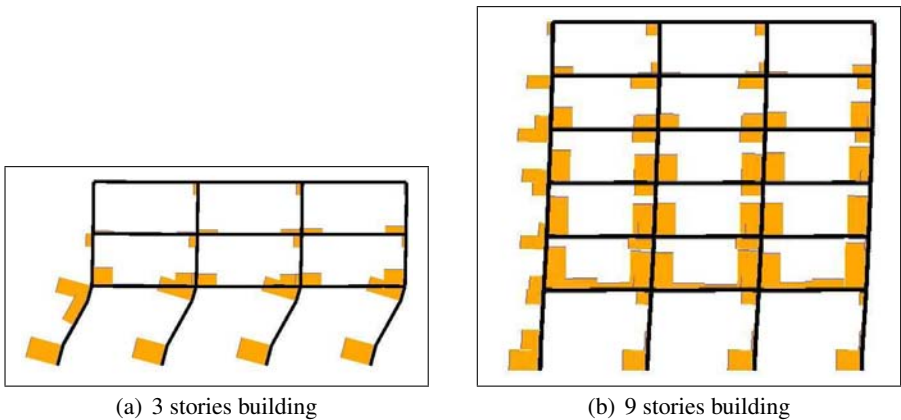(a) 3 stories building   (b) 9 stories building

Figure 8. Distribution of local damage-index at collapse displacement.

Figure 9 shows overstrength computed values for outer frames of the buildings under study, plotted in function of number of stories. Results clearly demonstrate that the influence of number of spans, equivalent to considering different numbers of resistant lines, is very low. In all cases, overstrength computed values are closer to each other. It can also be seen that these values of combined overstrength factors and redundancy are slightly lower than the value prescribed by ASCE-7 for design of ductile-framed buildings.

4.2.   Non Linear Dynamic Analysis

In order to evaluate the dynamic response of buildings, the IDA (Incremental Dynamic Analysis) procedure was applied. This procedure consists in performing time-history analysis for registered ground motions or for artificially synthesized accelerograms scaled in such a way of inducing increasing levels of inelasticity in each new analysis [25]. A set of six artificial accelerograms, com-
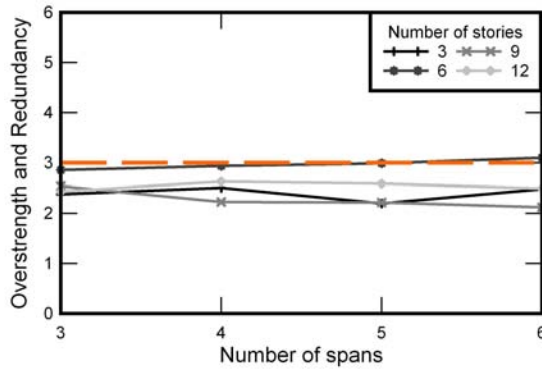
Figure 9. Overstrength and redundancy vs. number of stories.

patible with B type soil of the ASCE-7 elastic design spectrum, was generated, see Figure 10.
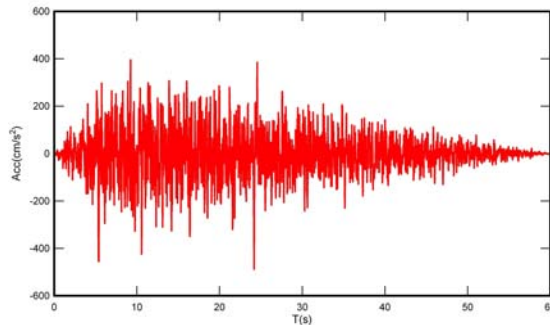

Figure 10. Synthesized accelerograms compatible with the ASCE-7 elastic design spectrum.

Figure 11 shows the elastic design spectrum and the 5% damping response spectra computed from the set of artificial accelerograms for the two levels of seismic hazard (0.3g and 0.4g) used in elastic design of buildings.

Peak acceleration equal to basic design acceleration is assumed in the analysis. Record is scaled from this value until a plastic response is reached by the structure; this procedure continues on and on until achieving collapse displacement. A maximum value of structural response is calculated for each value of scaled acceleration. IDA curves are obtained by plotting the earthquake peak
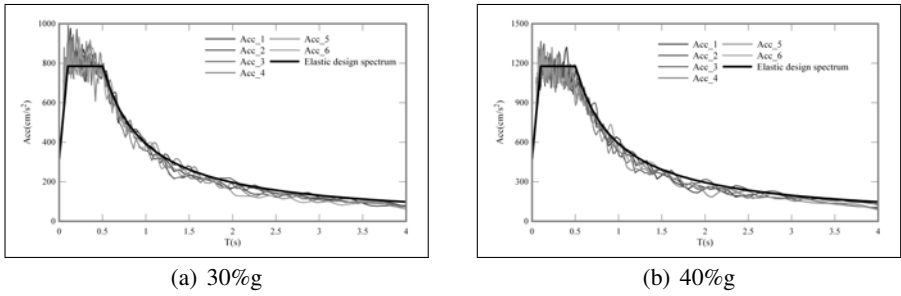
(a) 30%g (b) 40%g

Figure 11. Elastic design spectrum and response spectra.

acceleration in function of maximum value of the computed structural response. Collapse is reached when the capacity of the structure drops [9, 26, 27]. A usual criterion is to consider that collapse occurs whenever the slope of the curve is less than 20% of the elastic slope [25, 28]. Figure 12 shows IDA curves computed for the 3-span outer frame of the 3 storey building. Note that the collapse points of frames are closer to the values of the capacity curves.
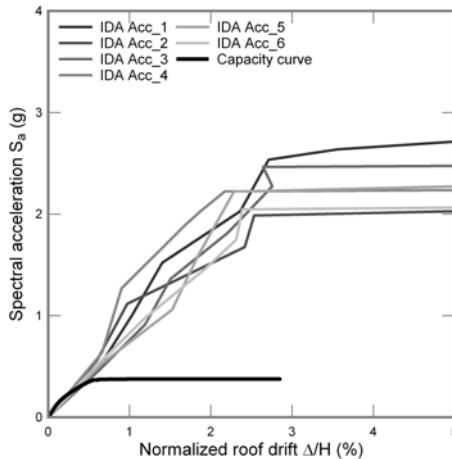

Figure 12. Set of IDA curves and capacity curve.

The dynamic analysis is useful to assess behavior factors q of the buildings. For this purpose the following equation has been proposed [4]:

Table 1. Computed behavior factors of outer frames (0.3g)

Number of storeys	$q_{equation}$	q_{code}	$\frac{q_{equation}}{q_{code}}$
3	19.70	8.00	2.46
6	16.45	8.00	2.05
9	15.46	8.00	1.93
12	16.09	8.00	2.01

$$q = \frac{a_{g(Collapse)}}{a_{g(Design_{yield})}} \tag{3}$$

where $a_{g(Collapse)}$ and $a_{g(Design_{yield})}$ are collapse and yielding design peak ground acceleration, respectively. The former is obtained from IDA curves and the latter is calculated from elastic analysis of the building. Average values of the q computed behavior factor of the buildings under study are shown in Table 1; these values correspond to the dynamic response obtained for the set of ten synthesized accelerograms, and are compared to behavior factors prescribed by the design codes.

Computed behavior factors show that, regardless of building height, seismic design performed by using the ACI318 leads to structures with satisfactory lateral capacity whenever subjected to strong motions.

4.3. Objective Damage Index

Some indexes measure the global seismic damage of a structure from its local damage, i.e. the contribution in a given instant of cumulative damage in structural elements to the structure being subject to seismic demand. Among the indexes which have served as baseline for many researches, it can be mentioned the one proposed by Park and Ang [29] which can determine damage in an element, based on non-linear dynamic response by the following expression:

$$DI_e = \frac{\delta_m}{\delta_u} + \frac{\beta}{\delta_u P_y} \int dE_h \tag{4}$$

where δ_m is the maximum displacement, δ_u is the ultimate displacement, β is a parameter adjusted depending on materials and structural type, P_y is the yield

strength and $\int dE_h$ is dissipated hysteretic energy. This damage-index is valid for an element at a local level; however, it is possible to apply this index for calculating the values for a specific structural level, or for the whole structure.

Another damage-index based on stiffness degradation is proposed by Gupta *et al.* [30]. They have formulated an expression based on the relationship between ultimate and yielding displacements, equivalent to ultimate and yielding stiffness. This formulation also includes a design ductility value according to:

$$DI = \frac{\frac{x_{maz}}{z_{00}} - 1}{\mu - 1} \tag{5}$$

A local damage-index is calculated using the PLCd finite element program with a constitutive damage and plasticity model enabling the correlation of damage with lateral displacements [16, 31]

$$D = 1 - \frac{\|P^{in}\|}{\|P_0^{in}\|} \tag{6}$$

where $\|P^{in}\|$ and $\|P_0^{in}\|$ are the norm of current and elastic values of the internal forces vectors, respectively. Initially, the material remains elastic and $D = 0$, but when all the energy of the material has been dissipated $\|P^{in}\| \to 0$ and $D = 1$.
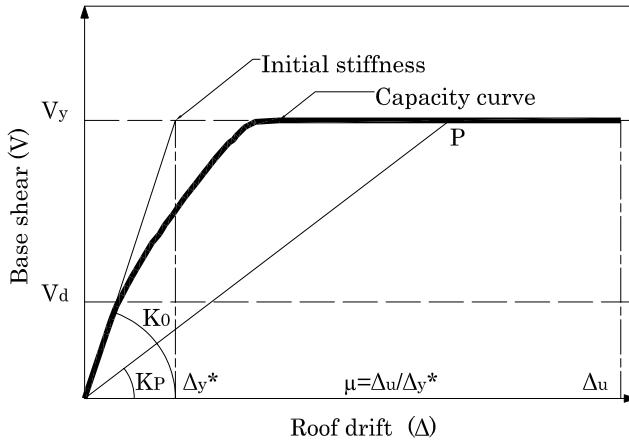

Figure 13. Parameters for determination of damage-index.

It is important to know the level of damage reached by a structure subject to certain demand. This is possible if the damage-index is normalized with respect

to the maximum damage which can occur in the structure [32]. This objective damage-index $0 \leq D \leq 1$ achieved by a structure at any P is defined as

$$D^P_{obj} = \frac{D_P}{D_C} = D_P \frac{\mu}{1-\mu} = \frac{(1-\frac{K_P}{K_0})\mu}{1-\mu} \qquad (7)$$

For example, for P point, which might be the performance point resulting from the intersection between inelastic demand spectrum and capacity curve (obtained from pushover analysis), it corresponds a stiffness K_P. Other parameters are initial stiffness K_0 and ductility μ, calculated by using yielding displacement Δ^*_y corresponding to the intersection of initial stiffness with maximum shear value (see Figure 13).

Objective damage-index is computed using Eq. 7, from the non-linear static analysis. Figure 14 shows evolution of objective damage-index respecting the normalized roof drift, computed for all frames of the 3 stories building. Curves are similar to those obtained for frames of the same number of stories.
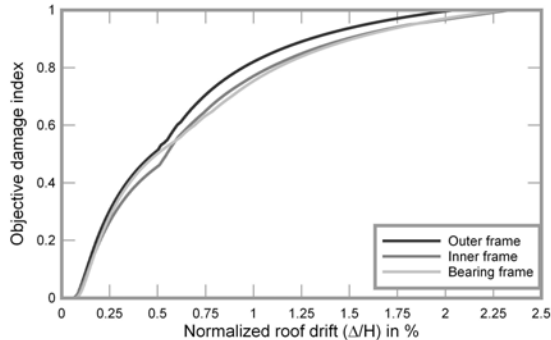

Figure 14. Evolution of damage-index of the 3 stories building.

5.   Seismic Safety

Nowadays, it is widely accepted among the scientific community that the Performance-Based Design is the most rational procedure. This requires definition of a set of Limit States in order to evaluate the damage that may be caused by earthquakes. These Limit States are frequently defined by engineering demand parameters, among which the most used are inter-story drift, global drift

and global structural damage. These demand parameters define damage thresholds associated with Limit States, which allows calculating fragility curves and damage probability matrices used in seismic safety assessment of buildings.

Consequently, it is necessary to select the evaluation criterion which represents the moment when the structure reaches a specific limit state. According to the above, interstory drift is a dimensionless value which quantifies properly the damage under lateral loads. Among published values, a set of inter-story drifts were selected from which specific damage reaches a threshold corresponding to a Limit State.

Damage thresholds are determined using the VISION 2000 procedure [33], in which they are expressed in function of interstory drifts. In this chapter, five damage state thresholds are defined both from interstory drift curve and from capacity curve. For the slight damage state, roof drift corresponding to an interstory drift of 0.5% is considered. Service damage state corresponds to the roof drift for which an interstory drift of 1% is reached in almost all the structure stories. Repairable damage state is defined by an inter-story drift of 1.5%. A severe damage state is identified by a roof drift producing a 2.0% of interstory drift at each level of the structure. Finally, a total damage state (collapse) corresponds to ultimate roof displacement obtained from the capacity curve. Mean values and standard deviation were computed from the non-linear response of buildings with the same geometric and structural type, with a variation of the number of spans from 3 to 6 [34, 35].
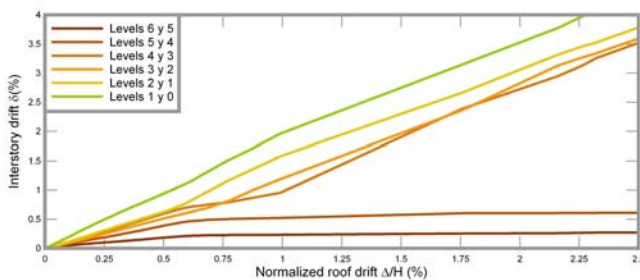

Figure 15. Determination of the damage thresholds.

To determine damage thresholds it is necessary to plot the evolution of interstory drifts with respect to global drift (roof displacement normalized with total building height). With this plot it is possible to obtain the global drift limit corresponding to a state i, characterized by interstory drift, see Figure 15. In

the case of a building with *n* levels, *n* evolution curves are obtained; global drift of a Limit State corresponding to the intersection of the first curve with the inter-story drift characterizing the Limit State.

Figure 16 Figure 16 shows the results obtained from outer frames of the 6 storey buildings designed for an acceleration of 0.3g. This figure shows that there is a clear dispersion of results for displacement at collapse, but these are kept within a range between 2.25% and 2.5%, compared to the values reported by Kircher *et al.* [36] and Dymiotis *et al.* [37], which are between 2% and 4%.
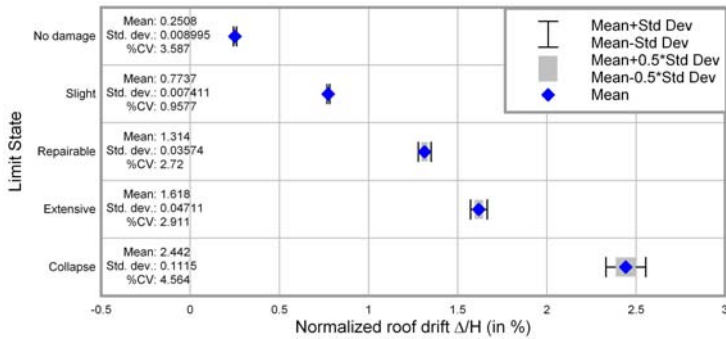

Figure 16. Mean and standard deviation for damage thresholds.

Figure 17 shows a comparison of results obtained by the above procedure with experimental results reported by Dymiotis *et al.* [37]. It can be seen that values obtained from non-linear analysis fit quite well with experimental values, regardless of the number of spans being considered.

Given this difference in results, Vielma *et al.* [34] have proposed the following expressions to determine interstory drifts δ (expressed in%) from normalized roof drifts of the buildings (Δ/H expressed in%)):

$$\delta = 0.1299 + 0.4358(\frac{\Delta}{H}) \qquad forN = 3$$

$$\delta = 0.1503 + 0.5256(\frac{\Delta}{H}) \qquad forN = 6$$

$$\delta = 0.06518 + 0.6280(\frac{\Delta}{H}) \qquad forN = 9 \tag{8}$$

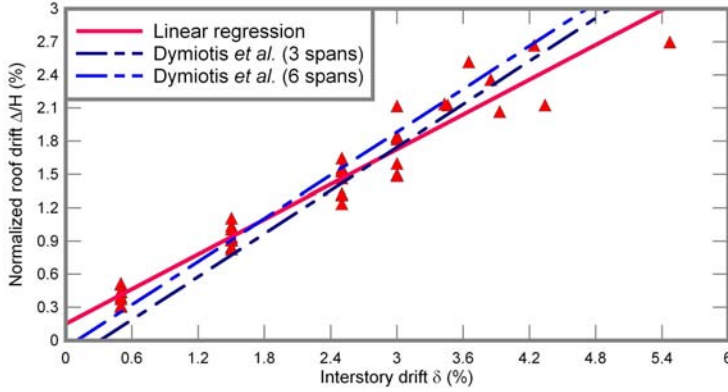$$\delta = 0.01184 + 0.6312(\frac{\Delta}{H}) \qquad forN = 12$$

Figure 17. Comparison of numerical and experimental results.

Figure 18 shows damage thresholds values applied to the capacity curve of the outer frame of the 3 level building, designed for acceleration of 0.3g. By using Equation 7, objective damage-indexes are calculated with thresholds associated to Limit States.

The combined use of thresholds and damage-indexes allows a quick characterization of the seismic response of a building and provides sufficient criteria for evaluating the behavior of a particular configuration or pre-design subject to specific demand buildings, e.g. the spectrum prescribed by the design code.

## 5.1.	Performance Point

In order to evaluate seismic safety of the buildings, the performance point represents an adequate measure. It is obtained by maximum drift of an equivalent single degree of freedom induced by the seismic demand. The points of all cases being studied have been determined by using the N2 procedure [38] which requires transformation of the capacity curve into a capacity spectrum, expressed in terms of spectral displacement, S_d and spectral acceleration, S_a. The former is obtained by means of equation

$$S_d = \frac{\delta_c}{MPF} \tag{9}$$

where δ_c is the roof displacement. The term *MPF* term is the modal participation factor calculated from the response in the first mode of vibration.
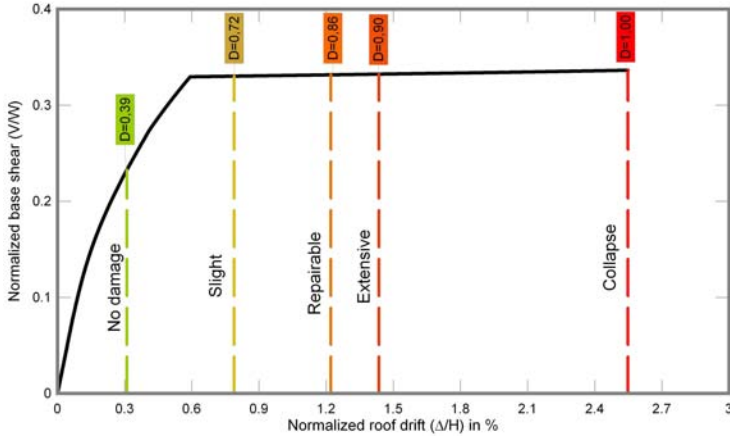
Figure 18. Damage thresholds with associated damage-index values.

$$MPF = \frac{\sum_{i=1}^{n} m_i \phi_{1,i}}{\sum_{i=1}^{n} m_i \phi_{1,i}^2} \qquad (10)$$

Spectral acceleration S_a is calculated by means of:

$$S_a = \frac{\frac{V}{W}}{\alpha} \qquad (11)$$

where V is the base shear, W is the seismic weight and α is a coefficient obtained as

$$\alpha = \frac{(\sum_{i=1}^{n} m_i \phi_{1,i})^2}{\sum_{i=1}^{n} m_i \phi_{1,i}^2} \qquad (12)$$

Figure 19 shows a typical capacity spectra crossed with the corresponding elastic demand spectrum. Idealized bilinear shape of the capacity spectra is also shown.

Spectral displacement values corresponding to performance point are shown in Table 2. An important feature influencing the non-linear response of buildings is the ratio between performance point displacement and collapse displacement. This ratio indicates whether the behavior of a structure is ductile or fragile. Lower values correspond to the 12-storey buildings, which have a weak-beam strong-column failure mechanism.
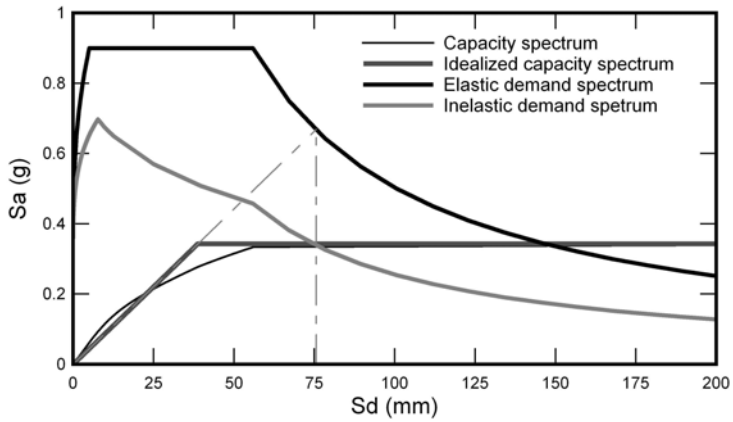
Figure 19. Determination of performance point.

Table 2. Roof drift of performance points for the studied buildings

Number of stories	Performance point (%)	Normalized roof drift		Ratio	
		Static analysis	Dynamic analysis (average)	Static analysis	Dynamic analysis (average)
3	0.71	2.93	2.52	0.24	0.28
6	0.47	2.41	2.65	0.20	0.18
9	0.44	2.58	2.67	0.17	0.17
12	0.28	2.49	2.70	0.11	0.10

5.2. Fragility Curves

Fragility curves are particularly useful for evaluating seismic safety of buildings. They are obtained by using spectral displacements determined for damage thresholds and considering a lognormal probability density function for spectral displacements which define damage states [39–42].

$$F(S_d) = \frac{1}{\beta_{ds} S_d \sqrt[n]{2\pi}} \exp[-\frac{1}{2}(\frac{1}{\beta_{ds}} \ln \frac{S_d}{\bar{S}_{d,ds}})^2] \qquad (13)$$

where $\bar{S}_{d,ds}$ is the mean value of spectral displacement for which the building reaches damage state threshold d_s and β_{ds} is the standard deviation of the natural logarithm of spectral displacement for damage state d_s. The conditional probability $P(S_d)$ of reaching or exceeding a particular damage state d_s, given the spectral displacement S_d, is defined as

$$P(S_d) = \int_0^S F(S_d)dS_d \qquad (14)$$

With fragility curves it is possible to calculate the values of probability of exceeding a particular limit state. Probabilities are calculated for a specific displacement or acceleration, usually obtained from a level of demand. Demand generally corresponds to the point of performance described in the previous subsection. Figure 20 shows fragility curves calculated for inner frames of the 3 and 12 storey buildings.

For more complete results the reader is referred to [27, 34, 35]

(a) Inner frame of the 3 stories building   (b) Inner frame of the 12 stories building
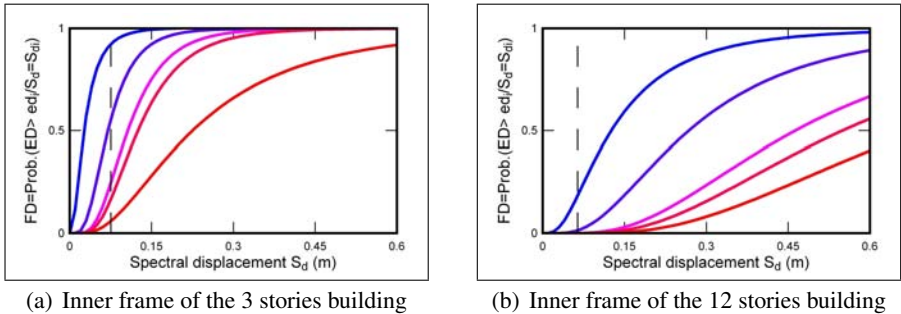
Figure 20. Fragility curves with performance point displacement.

Figure 21 shows damage probability matrices calculated for performance points achieved for inner frames of the 3 and 12 storey buildings. It is important to note that for frames of the same building, probabilities vary according to load ratio (seismic load/gravity load). Another important feature is the increasing values of probabilities that low rise buildings reach higher damage states; as discussed in previous sections, collapse of these buildings is associated with the soft-storey mechanism. For example, in the case of inner frames of the 3-level building, probability to reach collapse is four times higher than in the case of the outer frame of the same building. In contrast, 6, 9 and 12 storey buildings show very low probabilities to reach higher damage states, regardless of load ratio and

span number. For these buildings, predominant damage states are non-damage and slight damage.
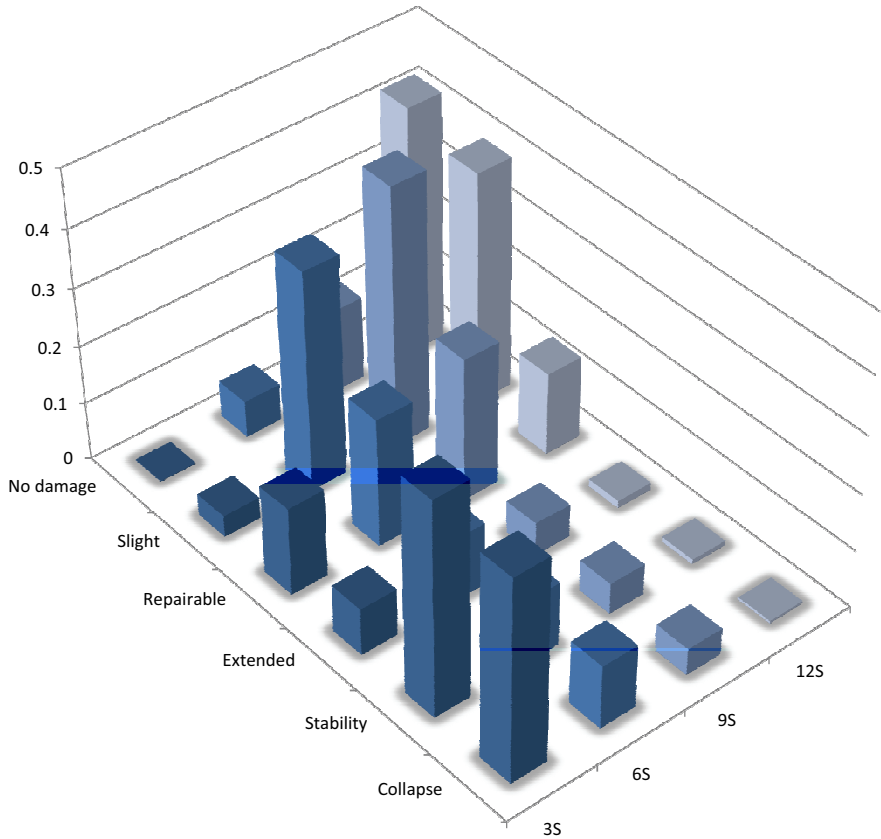

Figure 21. Damage probability matrices of outer frames.

Damage probability matrices contain the cumulative probability of reaching a specific limit state. This allows a qualitative assess of structural response during a specific seismic action. In Figure 21 it is possible to appreciate the probability matrices of internal frames, highlighting that frames of buildings with 3 levels have a probability of reaching more advanced stages of damage compared to frames of buildings of 6, 9 and 12 levels. This feature is repeated regardless of number of spans and location of frame. The difference in the response of low buildings is due to the fact that the failure mechanism of these

buildings is the soft story mechanism, in which damage is concentrated at the ends of columns in ground level, resulting in loss of global stability.

5.3.   Concluding Remarks

Steps in this chapter show the importance of non-linear analysis in the evaluation of seismic safety of buildings. By incorporating the characteristics of the constitutive non-linearity of materials (plasticity and damage) and geometric (large deformations and displacements) of the structure, it is possible to estimate adequately the design parameters prescribed in codes.

These parameters are applied based on the experience of scientists and engineers; therefore, their validation helps to improve understanding the behavior of structures subject to earthquakes.

In order to apply the non-linear analysis in the evaluation of buildings designed according to current earthquake-resistant codes (ACI-318, ASCE-7), a group of concrete-reinforced buildings have been selected. These buildings have been studied by applying static and dynamic procedures which have allowed calculating ductility and overstrength values and response-reduction factors. Overall, assessment has enabled the awareness that design parameters are adjusted appropriately to safety requirements.

In the study, all parameters except overstrength values are higher than those prescribed by the design code. Computed values are slightly lower than those prescribed in the ASCE-7. Overstrength values are often interpreted as safety factors by some designers.

Among the assessment procedures explained, one is the verification of the appropriateness of applying the objective damage-index as a tool to quickly evaluate overall performance of structures when they are subject to a specific seismic demand.

Analyses applied demonstrated that although buildings are designed to apply the same special requirements to ensure adequate seismic performance, the safety exhibited by these buildings is not the same. This can be verified by observing the fragility curves obtained for buildings of 3 and 12 levels, where the first are more likely to reach advanced stages of damage. This feature is due to the failure mode characteristic of low buildings that corresponds to a soft-story mechanism.

References

[1] ACI, *Building code requirements for structural concrete,* (ACI318-05). Detroit: American concrete institute, 1st ed., 2005.

[2] PLCd, *Non-linear thermo mechanic finite element oriented to PhD student education.* Barcelona: CIMNE, 1st ed., 2008.

[3] ASCE, *Minimum Design Loads for Buildings and Other Structures.* Reston: American Society of Civil Engineers, 1st ed., 2005.

[4] A. M. Mwafi and A. Elnashai, "Calibration of force reduction factors of RC buildings," *J Earthq Eng*, vol. 6(2), pp. 239–273, 2002.

[5] A. M. Mwafi and A. Elnashai, "Overstrength and force reduction factors of multistory reinforced-concrete buildings," *Struct des tall buil*, vol. 11, pp. 329–351, 2002.

[6] L. Sanchez and A. Plumier, "Parametric study of ductile moment-resisting steel frames: a first step towards Eurocode 8 calibration," *Earthq Eng Struct D*, vol. 37, pp. 1135–1155, 2008.

[7] M. J. N. Priestley, G. M. Calvi, and M. J. Kowalski, *Displacement-based seismic design of structures.* Pavia Italy: IUSS Press, 1st ed., 2007.

[8] R. Park, "State-of-the-art report: ductility evaluation from laboratory and analytical testing," in *Proceedings of the 9th WCEE*, (Tokyo-Kyoto, Japan), pp. 605–616, IAEE, 1988.

[9] J. C. Vielma, A. H. Barbat, and S. Oller, "Seismic performance of waffle slabs buildings," *P I Civil Eng-Str B*, vol. 162, pp. 169–182, 2009.

[10] S. Oller and A. H. Barbat, "Moment-curvature damage model for bridges subjected to seismic loads," *Comput Methods Appl Mech Engrg*, vol. 195, pp. 4490–4511, 2006.

[11] E. Car, S. Oller, and E. Oñate, "A large strain plasticity for anisotropic materials: Composite material application," *Int J Plasticity*, vol. 17(11), pp. 1437–1463, 2001.

[12] P. Mata, S. Oller, and A. H.Barbat, "Static analysis of beam structures under nonlinear geometric and constitutive behaviour," *Comput Methods Appl Mech Engrg*, vol. 196, pp. 4458–4478, 2007.

[13] P. Mata, S. Oller, and A. H.Barbat, "Dynamic analysis of beam structures under nonlinear geometric and constitutive behaviour," *Comput Methods Appl Mech Engrg*, vol. 197, pp. 857–878, 2008.

[14] S. Oller, E. Oñate, J. Oliver, and J. Lubliner, "Finite element non-linear analysis of concrete structures using a plastic-damage model," *Eng Fract Mech*, vol. 35(1-3), pp. 219–231, 1990.

[15] J. Lubliner, J. Oliver, S. Oller, and E. Oñate, "A plastic-damage model for concrete," *Int J Solids Struct*, vol. 51, pp. 501–524, 1989.

[16] A. H. Barbat, S. Oller, E. Oñate, and A. Hanganu, "Viscous damage model for Timoshenko beam structures," *Int J Solids Struct*, vol. 34, pp. 3953–3976, 1997.

[17] J. Faleiro, S. Oller, and A. H. Barbat, "Plastic-damage seismic model for reinforced concrete frames," *Comput Struct*, vol. 86, pp. 581–597, 2008.

[18] S. Oller, E. Car, and J. Lubliner, "Definition of a general implicit orthotropic yield criterion," *Comput Meth Appl Mech Eng*, vol. 192(7-8), pp. 895–912, 2003.

[19] X. Martinez, F. Rastellini, S. Oller, and A. H.Barbat, "A numerical procedure simulating rc structures reinforced with FRP using the serial/parallel mixing theory," *Comput Struct*, vol. 86, pp. 1604–1618, 2008.

[20] O. Bayrak and S. Sheik, "Plastic hinge analysis," *J Struct Eng (ASCE)*, vol. 127, pp. 1092–1100, 2001.

[21] E. Spacone and S. El-Tawil, "Nonlinear analysis of steel-concrete composite structures: State of the art," *J Struct Eng (ASCE)*, vol. 126, pp. 159–168, 2000.

[22] Y. Shao, S. Aval, and A. Mirmiran, "Fiber-element model for cyclic analysis of concrete-filled fiber reinforced polymer tubes," *J Struct Eng (ASCE)*, vol. 131, pp. 292–303, 2005.

[23] J. C. Simo, "A finite strain beam formulation. The three-dimensional dynamic problem part I," *Comput Methods Appl Mech Engrg*, vol. 49, pp. 55–70, 1985.

[24] J. B. Mander, M. J. N. Priestley, and R. Park, "Observed stress-strain behaviour of confined concrete," *J Struct Eng (ASCE)*, vol. 114, pp. 1827–1849, 1988.

[25] D. Vamvatsikos and C. A. Cornell, "Incremental dynamic analysis," *Earthq Eng Struct D*, vol. 31(3), pp. 491–514, 2002.

[26] S. Kunnath, *Earthquake engineering for structural design*. Boca Raton: CRC Press, 1st ed., 2005.

[27] J. C. Vielma, A. H. Barbat, and S. Oller, "Seismic safety of low ductility buildings used in Spain," *Bull Earthquake Eng*, vol. 8, pp. 135–155, 2010.

[28] S. W. Han and A. Chopra, "Approximate incremental dynamic analysis using the modal pushover analysis procedure," *Earthq Eng Struct D*, vol. 35(3), pp. 1853–1873, 2006.

[29] Y. J. Park and A. H.-S. Ang, "Mechanistic seismic damage model for reinforced concrete," *J Struct Eng (ASCE)*, vol. 111, pp. 722–739, 1985.

[30] P. S. Gupta, S. R. Nielsen, and P. H. Kierkegaard, "A preliminary prediction of seismic damage-based degradation in RC structures," *Earthq Eng Struct D*, vol. 30, pp. 981–933, 2001.

[31] E. Car, S. Oller, and E. Oñate, "An anisotropic elastoplastic constitutive model for large strain analysis of fiber reinforced composite materials," *Comput Meth Appl Mech Eng*, vol. 185(2-4), pp. 245–277, 2000.

[32] J. C. Vielma, A. H. Barbat, and S. Oller, "An objective seismic damage index for the evaluation of the performance of RC buildings," in *Proceedings of the 14th WCEE*, (Beijing, China), IAEE, 2009.

[33] SEAOC, *Vision 2000 Report on Performance Based Seismic Engineering of Buildings*. Sacramento, California, USA: Structural Engineers Association of California, 1st ed., 1995.

[34] J. C. Vielma, A. H. Barbat, and S. Oller, "Umbrales de daño para esta-
dos límite de edificios porticados de concreto armado diseñados conforme
al ACI-318/IBC-2006," *Revista Internacional de Desastres Naturales*,
vol. 8, pp. 119–134, 2009.

[35] J. C. Vielma, *Caracterización de la respuesta sísmica de edificios de
hormigón armado mediante la respuesta no lineal*. PhD thesis, Techni-
cal University of Catalonia, 2008.

[36] C. Kircher, A. Nassar, O.Kustu, and W. Holmes, "Development of build-
ing damage functions for earthquake loss estimation," *Earthq Spectra*,
vol. 13(4), pp. 663–682, 1997.

[37] C. Dymiotis, A. Kappos, and M. Chrissanthopoulos, "Seismic reliability
of RC frames with uncertain drift and member capacity," *J Struct Eng
(ASCE)*, vol. 125(9), pp. 1038 – 1047, 1999.

[38] P. A. Fajfar, "Nonlinear analysis method for performance based seismic
design," *Earthq Spectra*, vol. 16(3), pp. 573–591, 2000.

[39] P. E. Pinto, R. Giannini, and P. Franchin, *Seismic reliability analysis of
structures*. Pavia Italy: IUSS Press, 1st ed., 2006.

[40] A. H. Barbat, L. G. Pujades, and N. Lantada, "Seismic damage evalua-
tion in urban areas using the capacity spectrum method: application to
Barcelona," *Soil Dyn Earthq Eng*, vol. 28, pp. 851–865, 2008.

[41] A. H. Barbat, L. G. Pujades, and N. Lantada, "Performance of buildings
under earthquakes in Barcelona, Spain," *Comput.-Aided Civ. Infrastruct*,
vol. 21, pp. 573–593, 2006.

[42] N. Lantada, L. G. Pujades, and A. H. Barbat, "Vulnerability index and ca-
pacity spectrum based methods for urban seismic risk evaluation. a com-
parison," *Nat Hazards*, vol. 25(3), pp. 299–326, 1989.